

PACS numbers: 46.55.+d, 47.10.A-, 81.20.Wk, 81.40.Lm, 81.40.Pq, 83.50.-v

## Modelling and Simulation of the Plastic Flows in Metal

M. O. Kurin, O. O. Horbachov, A. V. Onopchenko, and T. V. Loza

*National Aerospace University 'Kharkiv Aviation Institute',  
17 Chkalov Str.,  
UA-61070 Kharkiv, Ukraine*

One of the most important problems in cutting theory is modelling behaviour of cut material accompanied by significant plastic deformations. Determination the chip patterns formation allows to build a theory of entire complex of processes and phenomena occurring in cutting zone. Various schemes, methods and types of processing define a wide variety of implementation schemes with a wide range of orientation cutting edge relative to velocity vector of main working movement. In this regard, it becomes necessary to analyse basic schemes of metal flow around plate. Combination of various schemes can be used to obtain any processing scheme using the principle of superposition. Before, we have developed a new method constructing velocity fields, which is devoid of drawbacks and contradictions of other methods determining the displacements velocity fields. Thus, it becomes necessary to obtain particle velocity fields for basic schemes using the hyperbola method.

**Key words:** hyperbola method, plastic deformation, potential flow, velocity fields, vortex flow.

Однією з найважливіших проблем теорії різання є моделювання поведінки матеріалу, що зрізується при різанні, що супроводжується значними пластичними деформаціями. Визначення утворення стружки дає можливість побудувати теорію всього комплексу процесів і явищ, що відбуваються в зоні різання. Різноманітні схеми, методи та види оброблення визначають різноманітні схеми реалізації з широким діапазоном орієнтації ріжучої кромки відносно вектора швидкості основного робочого руху. У зв'язку з цим виникає необхідність проаналізувати основні схеми обтікання металу навколо пластини. Комбінація різних схем може бути ви-

Corresponding author: Oleksiy Oleksandrovych Horbachov  
E-mail: o.horbachov@khai.edu

Citation: M. O. Kurin, O. O. Horbachov, A. V. Onopchenko, and T. V. Loza, Modelling and Simulation of the Plastic Flows in Metal, *Metallofiz. Noveishie Tekhnol.*, **44**, No. 6: 785–806 (2022). DOI: [10.15407/mfint.44.06.0785](https://doi.org/10.15407/mfint.44.06.0785)

користана для одержання будь-якої схеми оброблення за принципом суперпозиції. Раніше нами була розроблена нова метода побудови полів швидкості, яка позбавлена недоліків і протиріч інших метод визначення переміщень полів швидкостей. Таким чином, виникає необхідність одержати поля швидкості частинок для базових схем методою гіперболи.

**Ключові слова:** метода гіперболи, пластична деформація, потенційний потік, поля швидкостей, вихровий потік.

*(Received February 24, 2022; in final version, May 2, 2022)*

## 1. INTRODUCTION

The most important general problem of any type machining of metals is to determine the main technological parameters, which include energy-power characteristics, such as deforming force, work, power, as well as the optimal parameters of the processing mode. Metal forming operations [1] are distinguished by the importance of such components as the maximum allowable degree of deformation workpiece [2], as well as its shape and initial dimensions [3].

The optimal technological parameters of mode turning [4], milling and drilling [5] should be understood as such processing parameters that, at maximum productivity [6], guarantee at least required quality of products [7], and ideally, the most favourable characteristics of the surface layer [8], providing an increase in resource characteristics and levelling negative impact of technological heredity [9] of previous operations. Real technological processes have operations [10] in which processing modes can rarely be called optimal [11], so the need to ensure quality of surface layer [12] forces us to assign processing modes to detriment of productivity [13], especially in grinding operations.

Determination of energy-power characteristics is fundamental to purpose of technological processing modes [14], therefore, the choice of equipment and equipping the operation, as well as the parts obtained quality depends on the magnitude of these factors [15]. Calculation of the power characteristics cannot be carried out without determining stress-strain state of the metal during processing [16]. Based on above considerations, it can be concluded that in order to effectively predict the power characteristics of various processes and operations of pressure, rolling and cutting, it is necessary to develop mathematical models reflecting relationship between functional characteristics of process and technological parameters of the processing modes. Correct construction of model is possible if a structural and logical scheme. One determines the methods and sequence of theoretical and experimental studies. The most suitable methods for calculating plastic deformation processes are methods based on a closed system equations of continuum mechanics [17]. In this case, the deformed metal is consid-

ered as an idealized continuous medium [18] with averaged mechanical properties of a real metal. In fact, a four-dimensional space is introduced to describe the deformation process. The deformation process as a whole can be described by introducing function of four variables describing the field of displacement velocities. In most cases, solving applied technological problems for constructing desired velocity field, one can do with functions of two or three variables, especially when describing stationary processes. Analysis of process kinematics and initial prerequisites, as well as a rational choice of the coordinate system make it possible to quickly obtain displacement velocity field. Calculating stress-strain state of the metal and energy-power characteristics is based on velocity field.

## 2. LITERATURE REVIEW. FORMULATION OF THE PROBLEM

The chip formation process, which ensures the formation of a new surface, is accompanied by significant elastoplastic deformations, deformation rates, friction forces along the front and rear surfaces of the tool, build-up, an increase in hardness of deformable metal layers and significant heat release in the contact zone [19]. The emergence and development of mechanical, thermal and thermomechanical phenomena in the cutting zone is accompanied by occurrence of such important contact processes as adsorption, adhesion, desorption, redox processes, thermal destruction of cutting fluid, *etc.* This complex phenomenon has a significant impact on tool wear and the quality of the machined surface. [20]. Therefore, an important problem of cutting mechanics is to simulate behaviour of the cut layer during various technological processing operations, under conditions of significant plastic deformations.

A wide variety of geometric shapes of cutting inserts, which are widely used in modern cutting and differ in a wide range of angles and geometry of chip breakers, requires the construction of velocity fields that would describe the contact of removed chips with the wedge [21]. A detailed description of such contact requires a breakdown of the rake face of the tool into elementary components the pattern of velocity fields in the flow around which is known. Further, the subsequent construction of an integral picture is required, taking into account tool bit peculiarities and the kinematics of processing.

In the mechanics of a deformable body, a postulate is formulated [22], which reflects key requirement for the velocity fields of displacements in the plastic flow of metal. The essence of this postulate boils down to the following: the velocities field of particle displacement during plastic flow of metal, taking into account its incompressibility in considered region, should be solenoidal or vortex, which is mathematically expressed as follows:

$$\begin{cases} \nabla V = 0, \\ \nabla \times V = 0. \end{cases} \quad (1)$$

A large number of plotted particle displacement velocity fields that satisfy condition (1) have shown their effectiveness for investigation state of the material of a part and chips with various processing methods. Previously, we developed the hyperbole method [23] and noted its versatility, which makes it possible to solve a large class of problems in the analysis of deformation fields arising in deformation zone during various mechanical operations. Thus, the hyperbole method made it possible to effectively research the process of chip flow and its deformation when a wedge is introduced into the material for free and non-free cutting, as well as when an abrasive grain is introduced, which is important in the research of abrasive processing methods [24].

It is easy to see that direction of metal flow during deformation can be approximated by a hyperbola [25], just like flow of metal chips during cutting, if we analyse the macrostructure of the metal and direction of the fibres in part after forming processes [26]. At the same time, variety of metal forming operations [27] from dividing operations and punching to multi-strand stamping including the tools used in this case raise issue of finding an approximating flow curve for each operation individually. In most cases, the desired curve cannot be described by one branch of the hyperbola [28] (Fig. 1) within the selected coordinate system. As well, in certain operations of metal forming by pressure using tool the working surface of which or its part is a circle or an arc. In our opinion, all variety of metal production lines can be reduced to solving several problems that satisfactorily describe behaviour of the metal during deformation, namely: the flow around a wedge, plane and cylinder.

### 3. STRUCTURE OF INVESTIGATION OF ENERGY-POWER PARAMETERS OF MACHINING PROCESSES

An increase the efficiency of technological processes is inevitably associated with optimization of processing modes [29] and the prediction of power factors [30]. Many works are devoted to research the plastic flow of metal [31], the main results of which are presented in review [32].

The theoretical calculation of power factors is most rational to carry out according to methodology described in [33].

In this case, the deformable metal is considered as an idealized continuous medium with averaged mechanical properties of a real metal. Actually, in this instance, a four-dimensional space is introduced to describe the deformation process, and deformation process in general can be described by introducing function of four variables:

$$f(x, y, z, ct) = 0.$$

A theoretical analysis of the majority of technological processes along with the conducted experiments allows us to determine the nature of dependence velocity of particles plastic deformable metal on coordinates. The velocity of particles in four-dimensional space can be represented through a velocity vector:

$$\mathbf{V} = v_x \mathbf{i} + v_y \mathbf{j} + v_z \mathbf{k} + v_t \mathbf{n}. \tag{2}$$

The law constancy of a volume during the deformation is expressed by the continuity equation:

$$\text{div} \mathbf{V} = 0. \tag{3}$$

Using Eqs. (2) and (3), we can determine the form of functional dependence of speed on coordinates. Thus, the particles velocity field of material is determined, which makes it possible to calculate the strain rates and their intensity using the formulas:

$$\begin{aligned} \varepsilon_{q_1 q_1} &= \frac{1}{H_1} \frac{\partial V_{q_1}}{\partial q_1} + \frac{V_{q_2}}{H_1 H_2} \frac{\partial H_1}{\partial q_2} + \frac{V_{q_3}}{H_1 H_3} \frac{\partial H_1}{\partial q_3}, \\ \varepsilon_{q_1 q_2} &= \frac{1}{H_2} \frac{\partial V_{q_1}}{\partial q_2} + \frac{1}{H_1} \frac{\partial V_{q_2}}{\partial q_1} - \frac{V_{q_1}}{H_1 H_2} \frac{\partial H_1}{\partial q_1} - \frac{V_{q_2}}{H_1 H_2} \frac{\partial H_2}{\partial q_1}, \end{aligned} \tag{4}$$

where  $q_1, q_2,$  and  $q_3$  are orthogonal curvilinear coordinates.

In this case, the coupling equations hold:

$$x = x(q_1, q_2, q_3), \quad y = y(q_1, q_2, q_3), \quad z = z(q_1, q_2, q_3),$$

$$H_k = \sqrt{\sum_{i=1}^3 \left( \frac{\partial x_i}{\partial q_k} \right)^2}$$

— Lamé parameters,

$$\varepsilon_i = \frac{\sqrt{2}}{3} \sqrt{(\varepsilon_{q_1 q_2} - \varepsilon_{q_2 q_2})^2 + (\varepsilon_{q_2 q_2} - \varepsilon_{q_3 q_3})^2 + (\varepsilon_{q_3 q_3} - \varepsilon_{q_1 q_1})^2 + \frac{3}{2} (\varepsilon_{q_1 q_2}^2 + \varepsilon_{q_2 q_3}^2 + \varepsilon_{q_3 q_1}^2)}. \tag{5}$$

Next, it is necessary to determine components of deformation to find the energy-power process parameters:

$$e_{11} = \int \varepsilon_{11} dt, \quad e_{22} = \int \varepsilon_{22} dt,$$

and deformation intensity:

$$e_i = \frac{\sqrt{2}}{3} \sqrt{(e_{11} - e_{22})^2 + (e_{22} - e_{33})^2 + (e_{33} - e_{11})^2 + \frac{3}{2}(e_{12}^2 + e_{23}^2 + e_{31}^2)}.$$

An important characteristic machining processes is work of deformation which allows us to determine the power parameters. The total work of deformation is determined by integrating elementary work by volume:

$$A = \int \iiint_t \left( \rho V \frac{\partial V}{\partial t} + P_x \frac{\partial V}{\partial x} + P_y \frac{\partial V}{\partial y} + P_z \frac{\partial V}{\partial z} \right) dV dt. \quad (6)$$

Two functions were introduced in [5] by author. The first is called speed function:

$$L = \rho V \frac{\partial V}{\partial t}. \quad (7)$$

Part of equation (6) expresses the energy dissipation function:

$$E = P_x \frac{\partial V}{\partial x} + P_y \frac{\partial V}{\partial y} + P_z \frac{\partial V}{\partial z}. \quad (8)$$

The speed function is work aimed at increasing kinetic energy of elementary volume of metal in deformation process. The energy dissipation function is that part of work that take place into the material's own deformation. Taking into account (7) and (8), we rewrite equation (6) in the following form:

$$A = \int \iiint_t (L + E) dV dt. \quad (9)$$

If deformation is carried out at a low speed, then velocity function has a sufficiently small value in comparison with the energy dissipation function and can be neglected. In this case, work of deformation will be determined through the function of energy dissipation:

$$A = \int \iiint_t E dV dt. \quad (10)$$

Investigations in the deformation zone flow of deformed metal [34], especially in particular case of the formation and flow of chips [35] with different variants of flow around the cutting wedge [36], will allow constructing the initial velocity field, investigating in detail the stress-strain state in deformation zone and energy-force characteristics of the process. This approach will also make it possible to design model of the formation, development and annihilation of dislocations, which are the key to understanding the whole range of contact processes, such as hardening [37], adsorption, adhesion, *etc.*

### 3.1. Wedge Flows

For the convenience of work, the designations in parametric equations describing coordinates and velocity components will be marked with indices corresponding to position of curve in the plane quadrants. In this case, first number denotes the quadrant—beginning of movement along curve, and second—the end. The plastic flow of a metal upon penetration wedge into a rigid-plastic body has symmetry and geometric similarity relative to the axis of symmetry of the wedge, which is quite obvious and confirmed by recently developed model of crystal plasticity with gradient enhancement [38]. This flow is most typical for separation operations of metal forming or cutting.

The equation for branches of hyperbolas lying in quadrants 21 can be written by the system of equations:

$$\begin{cases} x_{21}(t) = a \sinh(\omega t + C) \cos \alpha + b \cosh(\omega t + C) \sin \alpha, \\ y_{21}(t) = -a \sinh(\omega t + C) \sin \alpha + b \cosh(\omega t + C) \cos \alpha. \end{cases} \quad (11)$$

where  $\omega$ ,  $C$  is some constants,  $t$  is time,  $a$  is semi-major axis, and  $b$  is semi-minor axis.

The components of speed movement are obtained by differentiating system (11) with respect to time [23]:

$$\begin{cases} V_{x_{21}}(t) = a\omega \cosh(\omega t + C) \cos \alpha + b\omega \sinh(\omega t + C) \sin \alpha, \\ V_{y_{21}}(t) = b\omega \sinh(\omega t + C) \cos \alpha - a\omega \cosh(\omega t + C) \sin \alpha. \end{cases} \quad (12)$$

The field of particle velocities during flow around edge of the wedge can be represented as:

$$\begin{cases} V_{x_{21}}(x, y) = V_0(\omega(x, y)(e^2 - 1))^{-1/2} [(x \cos \alpha - y \sin \alpha)e^2 \sin \alpha + y], \\ V_{y_{21}}(x, y) = V_0(\omega(x, y)(e^2 - 1))^{-1/2} [(x \cos \alpha - y \sin \alpha)e^2 \cos \alpha - x], \\ \omega(x, y) = \frac{e^2 \{x_0 \cos \alpha + [\sin^2 \alpha (1 - e^2) ((a(x, y))^2 (e^2 \sin^2 \alpha - 1) - x_0^2)]^{1/2}\}^2}{(1 - e^2 \sin^2 \alpha)^2 + (a(x, y))^2}, \\ a(x, y) = [(x \cos \alpha - y \sin \alpha)^2 e^2 - (x^2 + y^2)]^{1/2} (1 - e^2)^{-1/2}. \end{cases} \quad (13)$$

where  $V_0$  is cutting speed,  $e$  is eccentricity of hyperbola,  $x_0$  is coordinate determines the plastic flow beginning.

In order to obtain equation of the hyperbolas branches located in quadrants 34, it is necessary to change the signs to opposite in the equation  $y(t)$  of system (11), then we get:

$$\begin{cases} x_{34}(t) = a \sinh(\omega t + C) \cos \alpha + b \cosh(\omega t + C) \sin \alpha, \\ y_{34}(t) = a \sinh(\omega t + C) \sin \alpha - b \cosh(\omega t + C) \cos \alpha. \end{cases} \quad (14)$$

System (12) will take the form:

$$\begin{cases} V_{x_{34}}(t) = a\omega \cosh(\omega t + C) \cos \alpha + b\omega \sinh(\omega t + C) \sin \alpha, \\ V_{y_{34}}(t) = a\omega \cosh(\omega t + C) \sin \alpha - b\omega \sinh(\omega t + C) \cos \alpha. \end{cases} \quad (15)$$

The field of particle velocities during flow around edge will take the form:

$$\begin{cases} V_{x_{34}}(x, y) = V_0(\omega(x, y)(e^2 - 1))^{-1/2}[(x \cos \alpha + y \sin \alpha)e^2 \sin \alpha - y], \\ V_{y_{34}}(x, y) = V_0(\omega(x, y)(e^2 - 1))^{-1/2}[-(x \cos \alpha - y \sin \alpha)e^2 \cos \alpha + x], \\ \omega(x, y) = \frac{e^2 \{x_0 \cos \alpha + [\sin^2 \alpha (1 - e^2)((a(x, y))^2 (e^2 \sin^2 \alpha - 1) - x_0^2)]^{1/2}\}^2}{(1 - e^2 \sin^2 \alpha)^2} + (a(x, y))^2, \\ a(x, y) = [(x \cos \alpha + y \sin \alpha)^2 e^2 - (x^2 + y^2)]^{1/2} (1 - e^2)^{-1/2}. \end{cases} \quad (16)$$

### 3.2. Flow around a Plate with Horizontal Component Only

The equation of hyperbola located in quadrants 21 is identical to the previously obtained system (1)–(3). To obtain equation for the branches of hyperbolas located in the 3<sup>rd</sup> quadrant in the form of system (11), we will use the following algorithm. First of all, in the adopted coordinate system, is necessary to change sign in equation  $y(t)$  of system (11), then it is necessary to take into account that true angle  $[\gamma] = \pi - \gamma$ , and the true one  $[\alpha] = -\pi/2 + \gamma/2$ , but taking into account that  $a = -\gamma/2$ ,  $[\alpha] = -\pi/2 - \alpha$ ,  $b_{33} = a \operatorname{tg}((\pi - \gamma)/2)$  is the hyperbola parameter. After substituting  $[\alpha]$  and  $b_{33}$  into system (11), we obtain the equations describing the desired trajectory of motion:

$$\begin{cases} x_{33}(t) = -a \sinh(\omega t + C) \sin \alpha - \frac{a^2}{b} \cosh(\omega t + C) \cos \alpha, \\ y_{33}(t) = -a \sinh(\omega t + C) \cos \alpha + \frac{a^2}{b} \cosh(\omega t + C) \sin \alpha. \end{cases} \quad (17)$$

Differentiating system (17) with respect to time, we obtain the speeds:



$$\begin{cases} V_{x33}(t) = -\omega[a \cosh(\omega t + C) \sin \alpha + \frac{a^2}{b} \sinh(\omega t + C) \cos \alpha], \\ V_{y33}(t) = \omega[\frac{a^2}{b} \sinh(\omega t + C) \sin \alpha - a \cosh(\omega t + C) \cos \alpha]. \end{cases} \tag{18}$$

Using the technique described in [23], we obtain from system (18) the velocity field in Euler coordinates:

$$\begin{cases} V_{x33}(x, y) = V_0(\omega(x, y)(e^2 - 1))^{-1/2}[\cos \alpha(x \sin \alpha + y \cos \alpha) - (e^2 - 1)y], \\ V_{y33}(x, y) = -V_0(\omega(x, y)(e^2 - 1))^{-1/2}[e^2 \sin \alpha(x \sin \alpha - y \cos \alpha) - (e^2 - 1)x], \\ \omega(x, y) = ((e^2 - 1)(e^2 \sin^2 \alpha - 1))^{-2} e^2 \{[\cos^2 \alpha(x_0^2(e^2 - 1) - (a(x, y))^2(1 - e^2 \sin^2 \alpha))]^{1/2} - x_0 \sin \alpha(e^2 - 1)\}^2 + (a(x, y))^2, \\ a(x, y) = \sqrt{(x^2 + y^2)(e^2 - 1) - (y \cos \alpha + x \sin \alpha)^2 e^2}. \end{cases} \tag{19}$$

### 3.3. Flow around a Plate with Vertical Component Only

To get the trajectory 23 from equations (11) describing the motion along the hyperbola, it is necessary to swap  $x(t)$  and  $y(t)$  and change sign in expressions to the opposite, then we get:

$$\begin{cases} x_{23}(t) = -(-a \sinh(\omega t + C) \sin \alpha_{23} + b_{23} \cosh(\omega t + C) \cos \alpha_{23}), \\ y_{23}(t) = -(a \sinh(\omega t + C) \cos \alpha_{23} + b_{23} \cosh(\omega t + C) \sin \alpha_{23}). \end{cases} \tag{20}$$

Evidently  $[\gamma] = \pi/2 - \gamma$  is valid angle, and  $[\alpha_{23}] = -[\gamma]/2 = -\pi/4 + \gamma/2 = -\pi/4 - \alpha$ ; hyperbola parameter  $b_{23} = a \operatorname{tg}(\pi/4 - \gamma/2) = a(a - b)/(a + b)$ . Then we get the equation:  $\sin \alpha_{23} = -2^{-1/2}(\cos \alpha + \sin \alpha)$  and  $\cos \alpha_{23} = 2^{-1/2}(\cos \alpha - \sin \alpha)$ . After substitution, system (20) will take the following form:

$$\begin{cases} x_{23}(t) = -\frac{\sqrt{2}a}{2} \sinh(\omega t + C)(\cos \alpha + \sin \alpha) - \\ -\frac{\sqrt{2}a(a - b)}{2(a + b)} \cosh(\omega t + C)(\cos \alpha - \sin \alpha), \\ y_{23}(t) = -\frac{\sqrt{2}a}{2} \sinh(\omega t + C)(\cos \alpha - \sin \alpha) + \\ +\frac{\sqrt{2}a(a - b)}{2(a + b)} \cosh(\omega t + C)(\cos \alpha + \sin \alpha). \end{cases} \tag{21}$$

The velocities will look like this:

$$\left\{ \begin{aligned} V_{x_{23}}(t) &= -\frac{\sqrt{2}\omega}{2} [a \cosh(\omega t + C)(\cos \alpha + \sin \alpha) + \\ &\quad + a \frac{a-b}{a+b} \sinh(\omega t + C)(\cos \alpha - \sin \alpha)], \\ V_{y_{23}}(t) &= \frac{\sqrt{2}\omega}{2} [a \frac{a-b}{a+b} \sinh(\omega t + C)(\cos \alpha + \sin \alpha) - \\ &\quad - a \cosh(\omega t + C)(\cos \alpha - \sin \alpha)]. \end{aligned} \right. \quad (22)$$

System (22) is transformed into the following:

$$\left\{ \begin{aligned} V_{x_{23}}(x, y) &= V_0(\omega(x, y))^{-1/2} (2 - e^2)^{-1} (-y \sin 2\alpha - x \cos 2\alpha)e^2 + 2y\sqrt{e^2 - 1}, \\ V_{y_{23}}(x, y) &= -V_0(\omega(x, y))^{-1/2} (2 - e^2)^{-1} (-x \sin 2\alpha + y \cos 2\alpha)e^2 - 2x\sqrt{e^2 - 1}, \\ \omega(x, y) &= \frac{((2 - e^2)Y_0(\sin \alpha + \cos \alpha) - (1 + \sqrt{e^2 - 1})\zeta(x, y))^2}{2(e^2 \sin 2\alpha - 2\sqrt{e^2 - 1})^2} \times \\ &\quad \times \frac{2e^2}{e^2 + 2\sqrt{e^2 - 1}} - (a(x, y))^2 \frac{e^2 - 2\sqrt{e^2 - 1}}{e^2 + 2\sqrt{e^2 - 1}}, \\ a(x, y) &= \left( \frac{2\sqrt{e^2 - 1}(x^2 + y^2) - e^2(\sin 2\alpha(x^2 - y^2) + 2xy \cos 2\alpha)}{e^2 - 2\sqrt{e^2 - 1}} \right)^{1/2}, \\ \zeta(x, y) &= ((1 - \sin 2\alpha)Y_0^2(e^2 + 2\sqrt{e^2 - 1}) - (a(x, y))^2(e^2 \sin 2\alpha - 2\sqrt{e^2 - 1}))^{1/2}, \end{aligned} \right.$$

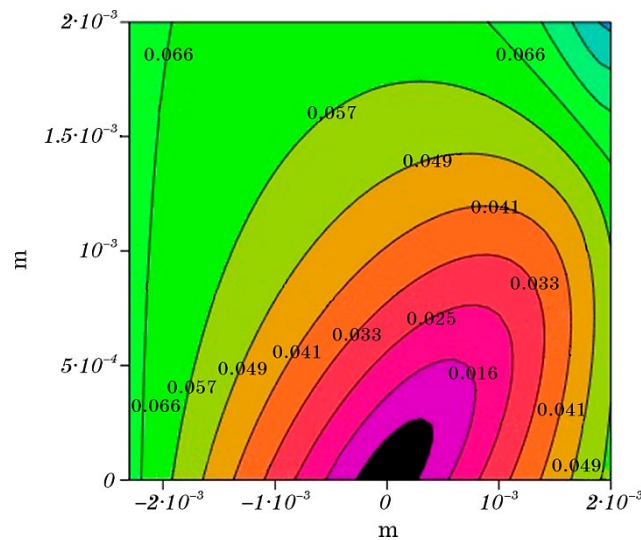


Fig. 1. Displacement velocity field around a wedge (top) quadrants 21.

where  $Y_0$  is coordinate determines the plastic flow beginning.

To describe the trajectory of movement 11, we use same technique, change  $y(t)$  to  $x(t)$  and change the sign of  $y(t)$  to the opposite:

$$\begin{cases} x_{11}(t) = -a \sinh(\omega t + C) \sin \alpha_{11} + b_{11} \cosh(\omega t + C) \cos \alpha_{11}, \\ y_{11}(t) = -(a \sinh(\omega t + C) \cos \alpha_{11} + b_{11} \cosh(\omega t + C) \sin \alpha_{11}). \end{cases} \quad (23)$$

In this case, the actual angle will be  $[\gamma] = \gamma + \pi/2$ , and  $[\alpha_{11}] = -(\pi/2 + \gamma)/2 = -\pi/4 - \gamma/2 = -\pi/4 + \alpha$ . Hyperbola parameter  $b_{11} = \text{atg}(\pi/4 + \gamma/2) = a(a + b)/(a - b)$ ,  $\sin \alpha_{11} = 2^{-1/2}(\sin \alpha - \cos \alpha)$  and  $\cos \alpha_{11} = 2^{-1/2}(\cos \alpha + \sin \alpha)$ . After substitution, we get:

$$\begin{cases} x_{11}(t) = \frac{\sqrt{2}a}{2} \sinh(\omega t + C)(\cos \alpha - \sin \alpha) + \\ + \frac{\sqrt{2}a(a + b)}{2(a - b)} \cosh(\omega t + C)(\cos \alpha + \sin \alpha), \\ y_{23}(t) = -\frac{\sqrt{2}a}{2} \sinh(\omega t + C)(\cos \alpha + \sin \alpha) + \\ + \frac{\sqrt{2}a(a + b)}{2(a - b)} \cosh(\omega t + C)(\cos \alpha - \sin \alpha). \end{cases} \quad (24)$$

The speed will look like:

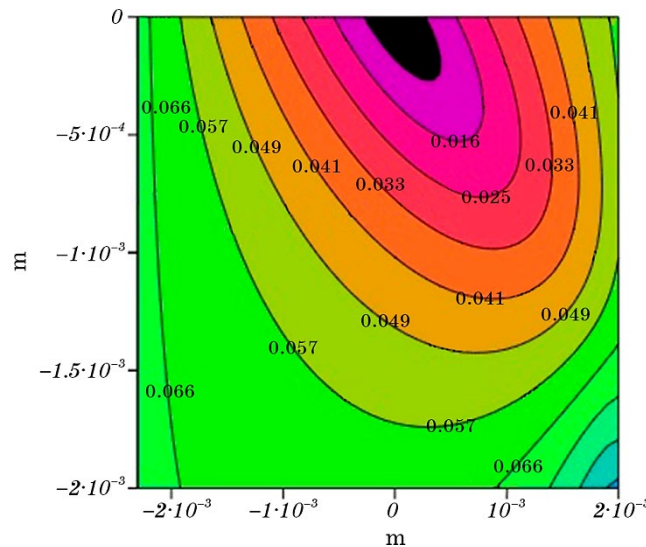


Fig. 2. Displacement velocity field around a wedge (bottom) quadrants 34.

$$\left\{ \begin{aligned} V_{x11}(t) &= \frac{\sqrt{2\omega}}{2} [a \cosh(\omega t + C)(\cos \alpha - \sin \alpha) + \\ &\quad + \frac{a(a+b)}{a-b} \sinh(\omega t + C)(\cos \alpha + \sin \alpha)], \\ V_{y11}(t) &= \frac{\sqrt{2\omega}}{2} [-a \cosh(\omega t + C)(\cos \alpha + \sin \alpha) + \\ &\quad + \frac{a(a+b)}{a-b} \sinh(\omega t + C)(\cos \alpha - \sin \alpha)]. \end{aligned} \right. \quad (25)$$

System (25) is transformed to the form:

$$\left\{ \begin{aligned} V_{x11}(x, y) &= V_0(\omega(x, y))^{-1/2} (2 - e^2)^{-1} (-y \sin 2\alpha - x \cos 2\alpha)e^2 + 2y\sqrt{e^2 - 1}, \\ V_{y11}(x, y) &= -V_0(\omega(x, y))^{-1/2} (2 - e^2)^{-1} (-y \cos 2\alpha + x \sin 2\alpha)e^2 - 2x\sqrt{e^2 - 1}, \\ \omega(x, y) &= ((2\sqrt{e^2 - 1} - e^2)Y_0(\sin \alpha + \cos \alpha) + (1 + \sqrt{e^2 - 1})(\cos \alpha - \\ &\quad - \sin \alpha)\zeta(x, y))^2 \frac{1}{2(e^2 \sin 2\alpha - 2\sqrt{e^2 - 1})^2} \frac{2e^2}{e^2 - 2\sqrt{e^2 - 1}} + (a(x, y))^2, \\ a(x, y) &= \left( \frac{-2\sqrt{e^2 - 1}(x^2 + y^2) + e^2(\sin 2\alpha(x^2 - y^2) + 2xy \cos 2\alpha)}{e^2 + 2\sqrt{e^2 - 1}} \right)^{1/2}, \\ \zeta(x, y) &= (Y_0^2(e^2 - 2\sqrt{e^2 - 1}) - (a(x, y))^2(e^2 \sin 2\alpha - 2\sqrt{e^2 - 1}))^{1/2}. \end{aligned} \right. \quad (26)$$

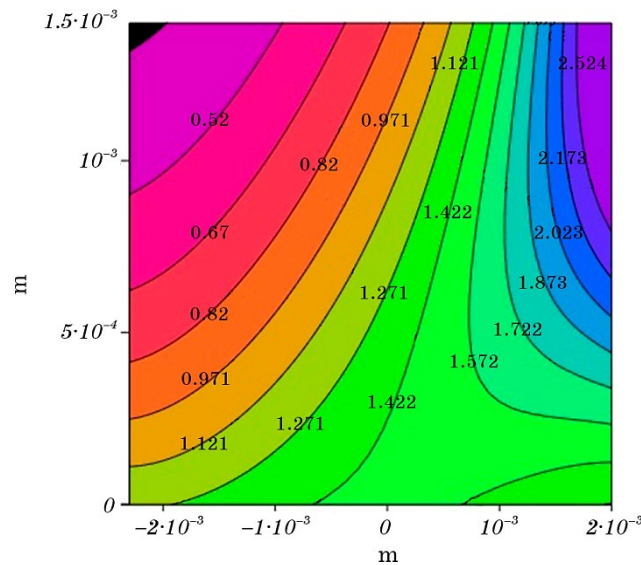


Fig. 3. Deformation intensity around a wedge (top) quadrants 21.

#### 4. INVESTIGATION MATERIAL DEFORMATION PROCESS IN CUTTING ZONE

The systems equations of displacement velocity field above satisfy condition (1) obtained by us, which is quite easy to verify by performing appropriate calculations. Here and below for cases we have got considered will not give intermediate analytical expressions due to the bulkiness of the expressions obtained. We will only outline sequence of mathematical operations that allow us to determine the important physical quantities characterizing the deformed state of chip material.

Based on displacement velocity field, it is easy to calculate a strain rate component, which in the case of specifying the velocity field in Cartesian coordinates, can be calculated using the dependencies:

$$\begin{aligned} \varepsilon_{xx} &= \frac{\partial V_x}{\partial x}, \varepsilon_{yy} = \frac{\partial V_y}{\partial y}, \varepsilon_{xy} = \frac{\partial V_x}{\partial y} + \frac{\partial V_y}{\partial x}, \\ \varepsilon_{zz} &= \frac{\partial V_z}{\partial z}, \varepsilon_{yz} = \frac{\partial V_y}{\partial z} + \frac{\partial V_z}{\partial y}, \varepsilon_{zx} = \frac{\partial V_z}{\partial x} + \frac{\partial V_x}{\partial z}. \end{aligned} \tag{27}$$

Next, we determine the components of deformation for Cartesian coordinates

$$\begin{aligned} e_{xx} &= \int \varepsilon_{xx} dt, e_{yy} = \int \varepsilon_{yy} dt, e_{xy} = \int \varepsilon_{xy} dt, \\ e_{zz} &= \int \varepsilon_{zz} dt, e_{yz} = \int \varepsilon_{yz} dt, e_{zx} = \int \varepsilon_{zx} dt. \end{aligned} \tag{28}$$

Complexes of formulas (27) and (28) allow calculating the intensities

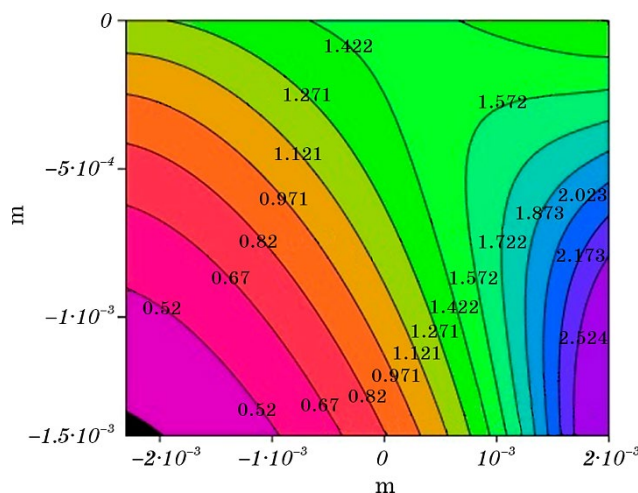


Fig. 4. Deformation intensity around a wedge (bottom) quadrants 34.

of strain rates and strain in Cartesian coordinates:

$$\varepsilon_i = \frac{\sqrt{2}}{3} \sqrt{(\varepsilon_{xx} - \varepsilon_{yy})^2 + (\varepsilon_{yy} - \varepsilon_{zz})^2 + (\varepsilon_{zz} - \varepsilon_{xx})^2 + \frac{3}{2}(\varepsilon_{xy}^2 + \varepsilon_{yz}^2 + \varepsilon_{zx}^2)},$$

$$e_i = \frac{\sqrt{2}}{3} \sqrt{(e_{xx} - e_{yy})^2 + (e_{yy} - e_{zz})^2 + (e_{zz} - e_{xx})^2 + \frac{3}{2}(e_{xy}^2 + e_{yz}^2 + e_{zx}^2)}. \quad (29)$$

It is enough in the first approximation to analyse displacement velocities field and deformation intensities field to assess the deformed state of material. Let us carry out calculation and construction the fields of displacement velocities and deformation intensities for specific processing conditions. The specified geometric shapes tool interaction modelling will be carried out under identical initial technological conditions. As an example, let us take the processing modes typical for operation of broaching grooves in heat-resistant alloys. Consider the deformation process material in contact with the tool in the form of wedge-plane at a processing speed  $V = 4$  m/min. In order to obtain a more visual picture and convenience of analysis, we will choose the tilt angle of working planes for wedge and plate section at velocity horizontal component  $\gamma = 60^\circ$  (streamlines 21, 34 and 33). To describe the plastic flow of metal along streamlines 11 and 23, we take  $\gamma = 30^\circ$ . The plastically deformed zone boundaries, as well as the length of contact of chips with plate front surface are:  $|X_0| = |Y_0| = 2.23 \cdot 10^{-3}$  m,  $C \approx 0.2 \cdot 10^{-3}$  m. The deformation intensity calculation is performed at

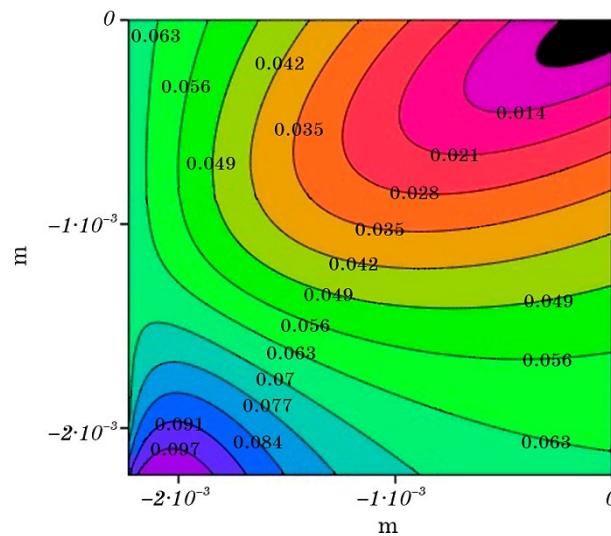
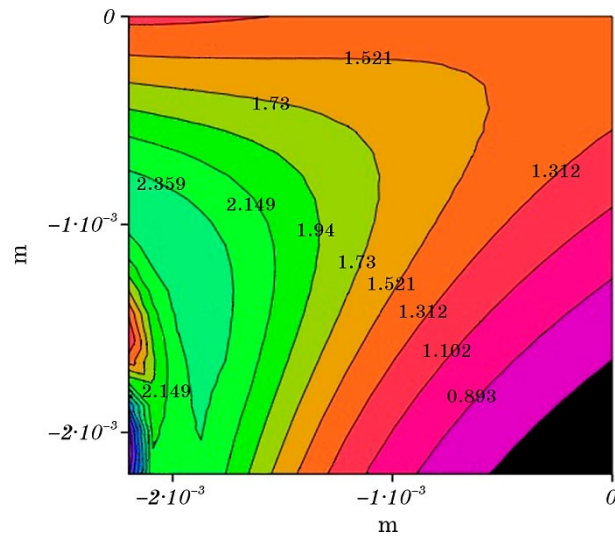


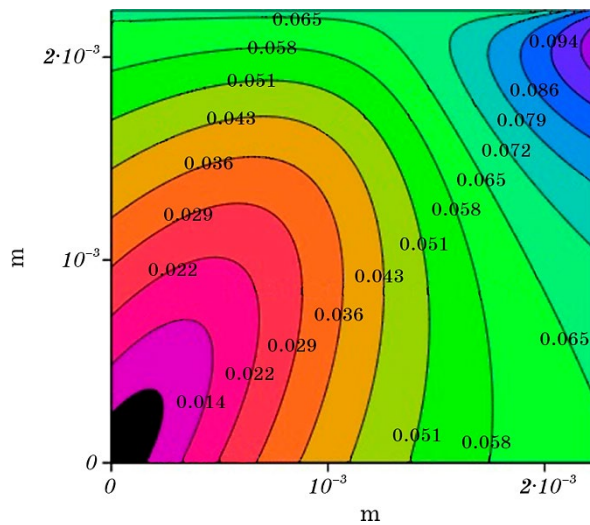
Fig. 5. Displacement velocity field around a plate (horizontal component) quadrants 33.



**Fig. 6.** Deformation intensity around a plate (horizontal component) quadrants 33.

the final moment of time  $t_k = (|X_0| + C)/V$ .

Let's consider the plotted graphs in detail. It is most convenient to analyse the displacement velocity fields in parallel with deformations (Figs. 1–10). This approach ensures integral picture formation of the



**Fig. 7.** Displacement velocity field around a plate (vertical component) quadrants 11.



plastic flow of the metal. The streamlines of the displacement velocity fields for all consideration problems have a characteristic slope relative to the ordinate axis, corresponding to inclination plane angle (Figs. 1, 2, 5, 7, 9). For all cases, velocity modulus decrease is noted as we approach the origin of the coordinate system. This is explained by the deceleration of the metal against tool surface in directly contacting layers and a natural resistance decrease metal flow with distance from disturbance source, which is working part of the tool. The strain intensities field repeats tool geometry for all considered cases (Figs. 3, 4, 6, 8, 10). The highest deformation intensity corresponds to the lowest metal flow rate, which is explained by the much larger metal deformations near the shear plane.

Let us analyse in detail the features of obtained fields for each of tasks. Flowing around a wedge the fields of displacement velocities and deformation intensities have symmetry about the OX axis, the isolines inclination angle corresponds to angle wedge. At the start point  $|X_0|=|Y_0|=2.23 \cdot 10^{-3}$  m, the flow rate is equal to processing speed, which corresponds to undeformed material flow rate and it is consistent with the initial conditions.

The flow around plate at horizontal velocity component in octant 33 (Figs. 5, 6) also agrees with the physical concepts we are developing. This reduces speed as it approaches origin where the tool plane is located. The isolines of strain intensity field repeat flow lines material. The magnitude of deformations intensity is greater than in case of flow around a wedge (Figs. 3, 4), with similar technological processing parameters (angle of inclination working plane, coordinate beginning

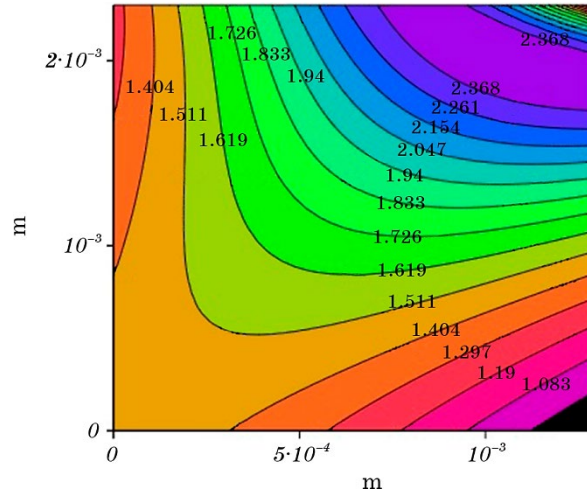
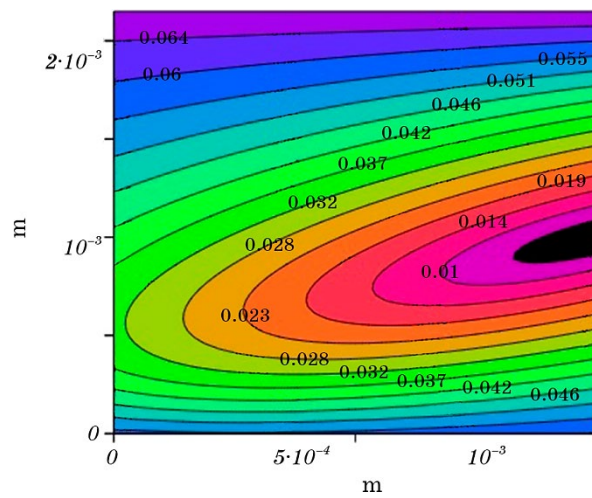


Fig. 8. Deformation intensity around a plate (vertical component) quadrants 11.

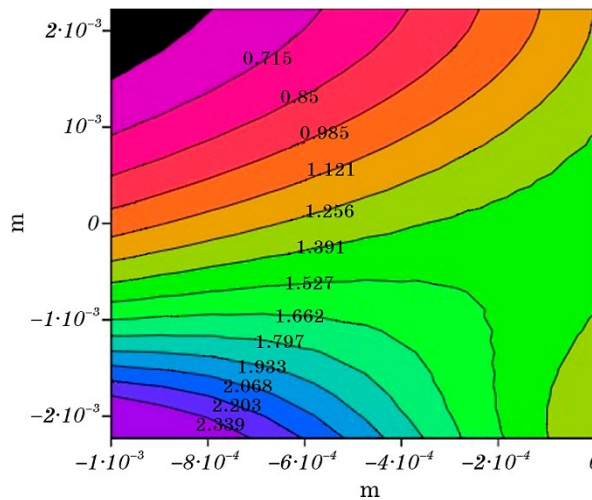




**Fig. 9.** Displacement velocity field around a plate (vertical component) quadrants 23.


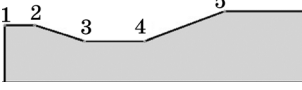

plastic deformation and processing speed). Indeed, the value of minimum deformation intensity at plate flow in octant 33 exceeds analogous value for the wedge by a factor of 1.5, while the core of maximum deformation is located not near tool surface, but near beginning of plastic flow plane.

The deformation increase in comparison with the wedge is explained



**Fig. 10.** Deformation intensity around a plate (vertical component) quadrants 23.

**TABLE 1.** Examples the displacements velocity field construction.

Machining process	Geometry of tool	Approximating line
Turning		12 hyperbola
		23 hyperbola
		12 hyperbola
		23 hyperbola
		34 hyperbola
		45 hyperbola
		12 hyperbola
	23 vortex or potential flow around cylinder	
	34 hyperbola	

by twofold greater angle of metal rotation of streamlines— $120^\circ$  versus  $60^\circ$  at wedge. The deformations highest intensity near the plane of deformation beginning is apparently a consequence of the pressure exerted by deformed metal layers along entire perimeter of maximum deformation zone, which in this regard can be considered a deformation core. Distance between deformation intensities isolines decreases precisely near the core of deformations maximum, which indicates the growth of function gradient most intensively in this field region. A more detailed analysis of the deformation mechanism of nucleus formation is possible when considering separately the deformation components.

At the vertical component of velocity (octant 11) the patterns of displacement velocities fields and deformation intensities are symmetric to fields of octant 33 relative to bisector of second and fourth octant central angles (Figs. 7, 8). The strain intensity field is also characterized by presence of deformation core bounded by a closed isoline. Nature values change is like octant 33. Flowing around a plane with a vertical component (23) the deformation rate fields are like flowing around part of a wedge (Fig. 9, 10). We can conclude that all fields have one of the types geometric symmetry (axial or rotational), which confirms correctness of our physical concepts.

Summing up, we can conclude that constructed fields of changes in functional parameters are consistent with physical concepts developed by us in this work, as well as with experimental studies.

Let's consider several examples of constructing displacement velocities field depending on the processing method and geometry of the tool working part (Table 1). At the heart of any cutting tool is a cutting wedge, the geometry of which varies in a wide range depending on the method and processing conditions. As we know the kinematics of metal flow is determined by the insert geometry and the processing speed. Therefore, there is no fundamental difference in processing method choice. It is enough to consider the flow around several chipbreakers of different geometries during turning.

Flow around plates sections formed by the broken line the metal streamlines are well approximated by the branches of hyperbolas. It is equally possible to use displacement velocity fields describing flow around both the potential and vortex cylinders to describe sections of circular arcs.

Developed technique can be applied to mathematical modelling [42], to solve assessing energy-power characteristics problems [43] behaviour structures during machining [44] and contact phenomena such as adsorption and adhesion in the processing zone during cutting.

## 5. CONCLUSION

Based on results of macrostructure analysis metal and direction of forgings fibres after various types of metal forming operations by pressure, the hyperbola method is proposed for displacement velocity fields constructing and analysing metal deformed state in processing zone. The structure for investigation of energy-power characteristics of metals mechanical processing is presented. It is shown that key system of equations are dependencies describing velocity fields of metal particles satisfy solenoidality requirement. An approach to description metal flow is proposed with various processing methods. The method essence consists in dividing tool working surface of complex geometry into flat and cylindrical shape sections. Problems modelling metal plastic flow are considered when flowing around a wedge; plate at vertical and horizontal components of speed; vortex and potential flow around the cylinder with ductile metal. On the hyperbola method, displacement velocity fields have been developed. It describes metal plastic flow at absolutely solid tool penetration into a rigid-plastic half-space. The material deformation process modelling is carried out for all solved problems under specific processing conditions. The fields of displacement velocities and deformation intensities are constructed. The features of metal flow are noted at modelling various problems. On the choice flowing around a cylindrical surface type general recom-

mentation are given at solving technological problems. Based on the simulation results, it can be concluded that functional parameters changes are consistent with physical concepts developed by us in work and experimental research. Several examples of displacement velocities field construction are considered depending on processing method and the tool working part geometry. For each case a sequence the approximating curves is proposed of streamline.

## REFERENCES

1. J. M. Allwood, S. R. Duncan, J. Cao, P. Groche, G. Hirt, B. Kinsey, T. Kuboki, M. Liewald, A. Sterzing, and A. E. Tekkaya, *CIRP Annals*, **65**: 573 (2016).
2. A. Topa and Q. H. Shah, *Int. J. Manufacturing Engineering*, **2014**: 385065 (2014).
3. E. Ghassemali, X. Song, M. Zarinejad, D. Atsushi, and M. J. Tan, *Handbook of Manufacturing Engineering and Technology* (Ed. A. Nee) (London: Springer: 2013).
4. X. Cui and J. Guo, *Int. J. Adv. Manuf. Technol.*, **96**: 4281 (2018).
5. G. M. Minquiz, V. Borja, M. López-Parra, A. C. Ramírez-Reivich, L. Ruiz-Huerta, R. C. Ambrosio Lázaro, A. S. Y. Sánchez, H. Vazquez-Leal, M.-E. Pavon-Solana, and J. Flores Méndez, *Mathematical Problems in Engineering*, **2020**: 8718597 (2020).
6. M. Sajgalik, A. Czan, M. Drbul, I. Danis, M. Miklos, O. Babik, and R. Joch, *Procedia Manufacturing*, **14**: 51 (2017).
7. S. Masoudi, M. J. Esfahani, F. Jafarian, and S. A. Mirsoleimani, *Int. J. Precis. Eng. and Manuf.-Green Tech.*, (2019).
8. Y. J. Lee and H. Wang, *Mater. Des.*, **192**: 108688 (2020).
9. B. Boswell, M. N. Islam, I. J. Davies, and A. Pramanik, *Proc. Institution Mech. Engineers, Part B: J. Engineering Manufacture*, **231**, Iss. 6: 913 (2017).
10. C. Baumgart, J. J. Radziwill, Fr. Kuster, and K. Wegener, *Procedia CIRP*, **58**: 517 (2017).
11. H. Jamshidi and E. Budak, *Procedia CIRP*, **77**: 299 (2018).
12. T. Zaborowski and R. Ochendusko, *Mechanik*, **10**: 135 (2017).
13. V. Larshin and N. Lishchenko, *Advances in Design, Simulation and Manufacturing* (Eds. V. Ivanov, Y. Rong, J. Trojanowska, J. Venus, O. Liaposhchenko, J. Zajac, I. Pavlenko, M. Edl, and D. Perakovic) (Springer: 2019), p. 79.
14. J. Badger, S. Murphy, and G. E. O'Donnell, *Int. J. Machine Tools Manufacture*, **125**: 11 (2018).
15. T. Jin, J. Yi, and P. Li, *Int. J. Adv. Manuf. Technol.*, **88**: 2609 (2017).
16. Yu. N. Alekseev, *Vvedenie v Teoriyu Obrabotki Metallov Davleniem, Prokatkoy i Rezaniiem* [Introduction to the Theory of Metal Processing via the Pressure, Rolling and Cutting] (Kharkiv: KhGU: 1969) (in Russian).
17. A. A. Kabatov, *Voprosy Proektirovaniya i Proizvodstva Konstruktsiy Letatel'nykh Apparatov*, **1**: 67 (2013) (in Russian).
18. A. A. Kabatov, *Tenologiya Almaznogo Vyglazhivaniya Detaley Aviatsionnykh Dvigatelay i Agregatov* [Technology for Diamond Smoothing of Aircraft Engine Parts and Units] (Thesis of Dissert. for PhD) (Kharkiv: National Aerospace University 'Kharkiv Aviation Institute': 2014) (in Russian).

19. J. M. Rodríguez, J. M. Carbonell, and P. Jonsén, *Arch. Computation Methods Eng.*, **27**: 387 (2020).
20. B. Li, *Int. J. Refractory Metals and Hard Materials*, **35**: 143 (2012).
21. T. Mabrouki, C. Courbon, Y. Zhang, J. Rech, D. Nélias, M. Asad, H. Hamdi, S. Belhadi, and F. Salvatore, *Comptes Rendus Mécanique*, **334**, Iss. 4–5: 335 (2016).
22. M. O. Kurin, *Metallofiz. Noveishie Tekhnol.*, **42**, No. 3: 433 (2020).
23. M. O. Kurin, *Metallofiz. Noveishie Tekhnol.*, **40**, No. 7: 859 (2018).
24. S. M. Nizhnik, *Tekhnologiya Shlifovaniya Detaley Aviatsionnykh Dvigatelye s Uchetom Uvelicheniya Aktivnoy Poverkhnosti Abrazivnogo Zerna* [Grinding Technology of Aviation Engine Parts, Taking into Account the Increase of the Active Surface of Abrasive Grain] (Thesis of Dissert. for PhD) (Kharkiv: National Aerospace University ‘Kharkiv Aviation Institute’: 2018) (in Russian).
25. B. Wang, Z. Li, M. Zheng, B. Zuo, J. Lin, and C. Zhu, *MATEC Web of Conferences*, **21**: 02005 (2015).
26. *Grain Flow in Forgings* (2021) <https://www.milwaukeeforge.com/grain-flow-in-forgings>.
27. *Cold Forging vs. Hot Forging—Considerations, Benefits and Drawbacks* (2014) <https://www.farinia.com/blog/cold-forging-vs-hot-forging-considerations-benefits-and-drawbacks>.
28. N. S. Mahesh, *Forging and Extrusion Processes* [https://asremavad.com/wp-content/uploads/2019/08/Forging-and-Extrusion-Processes\\_www.asremavad.com\\_.pdf](https://asremavad.com/wp-content/uploads/2019/08/Forging-and-Extrusion-Processes_www.asremavad.com_.pdf).
29. J. M. Allwood, T. H. C. Childs, A. T. Clare, A. K. M. De Silva, V. Dhokia, I. M. Hutchings, R. K. Leach, D. R. Leal-Ayala, S. Lowth, C. E. Majewski, A. Marzano, J. Mehnen, A. Nassehi, E. Ozturk, M. H. Raffles, R. Roy, I. Shyha, and S. Turner, *J. Materials Processing Technology*, **229**: 729 (2016).
30. S. Bolsunovsky, V. Vermel, and G. Gubanov, *Procedia CIRP*, **8**: 235 (2013).
31. L. B. Zuev, S. A. Barannikova, and A. G. Lunev, *Usp. Fiz. Met.*, **19**, No. 4: 379 (2018) (in Russian).
32. Yu. V. Milman, S. I. Chugunova, I. V. Goncharova, and A. A. Golubenko, *Usp. Fiz. Met.*, **19**, No. 3: 271 (2018).
33. M. O. Kurin, *Usp. Fiz. Met.*, **21**, No. 2: 249 (2020).
34. T. Sugihara, A. Udupa, and K. Viswanathan, *Mater. Trans.*, **60**, Iss. 9: 1436 (2019).
35. Okida Junya, Takuichiro Tayama, Yosuke Shimamoto, and Shinya Nakata. *SEI Technical Review*, **82**: 51 (2016).
36. V. P. Astakhov and S. Shvets, *J. Mater. Process. Technol.*, **146**: 193 (2004).
37. A. M. Korsunsky and M. Wiercigroch, *Int. J. Solids Struct.*, **47**: 1082 (2010).
38. M. Lewandowski and S. Stupkiewicz, *Int. J. Plasticity*, **109**: 54 (2018).
39. N. Ya. Fabrikant, *Aerodinamika* [Aerodynamics] (Moscow: Nauka: 1964) (in Russian).
40. L. G. Loytsyanskiy, *Mekhanika Zhidkosti i Gaza* [Mechanics of Fluid and Gas] (Moscow: Nauka: 1978) (in Russian).
41. A. I. Dolmatov, A. A. Kabatov, and M. A. Kurin, *Metallofiz. Noveishie Tekhnol.*, **35**, No. 10: 1407 (2013) (in Russian).
42. M. Dumas, D. Fabre, F. Valiorgue, G. Kermouche, A. Van Robaey, M. Girinon, A. Brosse, H. Karaoui, and J. Rech, *J. Materials Processing Technology*, **229**: 729 (2021).

43. V. Kombarov, V. Sorokin, Y. Tsegelnyk, S. Plankovskyy, Y. Aksonov, and O. Fojtů, *Int. J. Mechatronics Applied Mechanics*, **9**: 1 (2021).
44. S. Plankovskyy, V. Myntiuk, Y. Tsegelnyk, S. Zadorozhniy, V. Kombarov, *Mathematical Modeling and Simulation of Systems (MODS'2020)* (Eds. S. Shkarlet, A. Morozov, and A. Palagin,) (Springer: 2021), vol. **1265**, p. 82.